

Calcium aluminate cement in refractory applications: hydration kinetics of CA and CA₂

Sebastian Klaus¹, Andreas Buhr¹, Dagmar Schmidtmeier², Stefan Kuiper³

¹Almatis GmbH, Frankfurt, Germany, ²Almatis GmbH, Ludwigshafen, Germany,

³Almatis BV, Rotterdam, The Netherlands

Abstract

Calcium-mono-aluminate (CA or CaAl₂O₄) and calcium-di-aluminate (CA₂ or CaAl₄O₇) are the main phases in iron free high alumina cements (CAC) which are used in demanding refractory applications. It is well known that the hydraulic reactivity of calcium aluminate phases increases with the calcium content of the phase, and therefore CA shows higher reactivity than CA₂. Some literature even claims that CA₂ would be an almost inert phase with regard to hydraulic reactivity. This study investigates the hydration of pure CA and blends of CA and CA₂ using heat flow calorimetry and quantitative in-situ X-ray diffraction (QXRD) during hydration.

Heat flow was calculated by combining the QXRD data obtained during hydration of the mixes together with the standard enthalpies of formation of the participating phases. Comparing the observed heat flow from calorimetry with the heat flow calculated from QXRD data, good conformance could be obtained. The results show a clear pronounced influence of CA₂ on hydration of CAC and its heat of hydration during the first 22 hours. After more than 10 hours the hydration of CA₂ gives the major contribution to the heat flow.

Introduction

The hydration of calcium-mono-aluminate (CA) is part of several previous investigations and is well known. In common calcium aluminate cements (CAC) CA is the main hydraulic phase responsible for early strength development. Although recent investigations showed that CA reactivity can be increased by its fineness [1], it is worth having a closer look at CA₂ - the second main phase in most white CACs. CA₂ is known to be weakly hydraulic and was not of great interest in past investigations which looked into the hydration of CAC [2].

The hydration of synthesised CA and CA₂ in different ratios together with ZrSiO₄ as an inert filler, were investigated with isothermal heat flow calorimetry and in-situ X-ray diffraction. Through a combination of both methods the heat flow contributions of CA and CA₂ were evaluated.

Materials and methods

The reactive cement phases CA and CA₂ were synthesised from CaCO₃ (Sigma-Aldrich) and α-Al₂O₃ (Alpha Aesar). Inert ZrSiO₄ was added as a filler material to simulate a low cement castable concrete and to ensure good reproducibility [3]. Because of the very high specific surface area of the used ZrSiO₄ (d₅₀ = 0.2 μm) an actual water to cement ratio between 2.25 and 4.5 resulted.

The investigated model cement mixtures containing different contents (Tab. 1) of CA and CA₂ were investigated using heat flow calorimetry (quadruple design [4]) with a water to solid ratio (w/s-ratio) of 0.45. The in-situ XRD

measurements were performed on a D8 diffractometer equipped with a Lynx-Eye position sensitive detector (Bruker AXS). For XRD measurements the specimen was covered with a sheet of Kapton to prevent evaporation of water and to minimize CO₂ contamination during hydration. For both heat flow calorimetry and in-situ XRD measurements, the homogenised mixtures and the mixing water were equilibrated at 23±0.2°C. For all preparations a mixing time of 1 min was chosen.

Synthesized CAC	CA [wt.-%]	CA2 [wt.-%]	ZrSiO4 [wt.-%]
CAC-10/0	10	-	90
CAC-10/10	10	10	80
CAC-15/5	15	5	80

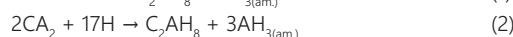
Table 1: Phase composition of investigated mixtures

The XRD data were evaluated with the G-factor method [5, 6] in combination with the Rietveld [7] refinement. The G-factor quantification is an external standard method which has the advantage that single crystalline phases can be quantified independently from other phases and especially from amorphous phases [8]. After O'Connor and Raven [9] the scale factor s_j of the phase j is directly proportional to the phase content c_j. The density of the phase is described as ρ_j and the cell volume by V_j. The mass attenuation coefficient μ* of the mixture (dry powder and water) can be evaluated from its known chemical composition [10]. The factor G is a constant reflecting the calibration of the measurement equipment and was frequently determined with a highly crystalline standard material (Si powder).

$$c_j = s_j \cdot \frac{\rho_j \cdot V_j^2 \cdot \mu^*}{G}$$

For further calculations the course of the quantitative X-ray diffraction (QXRD) data was fitted with the application Fityk [11].

Based on the fitted in-situ QXRD data and thermodynamic data from literature, the individual heat flow contributions of the hydration of CA and CA₂ was evaluated. For calculation of the heat of reaction (ΔH_r) the hydration reactions (1) and (2) were employed by using the enthalpies of formation in Tab. 2. A simultaneous hydration of the hydraulic phases and precipitation of the hydrate phases was assumed.



$$\Delta H_r(CA) = -693 \text{ J/g}$$

$$\Delta H_r(CA_2) = -498 \text{ J/g}$$

Phase	ΔH_f^0 [kJ/mol]	Reference
CA	-2323	Coughlin ^[12]
CA ₂	-4023	Hemmingway ^[13]
H	-286	Johnson et al. ^[14]
C ₂ AH ₈	-5433	Lothenbach et al. ^[15] , Matschei et al. ^[16]
AH ₃	-2578	Matschei et al. ^[16]

Table 2: Enthalpies of formation used for calculation of the heat flow

The calculated heat flow can be determined by combining the derivative established by fitted QXRD data of CA and CA₂ (dPhaseXRD) with the heat of reactions:

$$HF = \frac{1}{100} \cdot \frac{dPhaseXRD}{dt} \cdot \frac{\Delta H_R}{3.6} \cdot (-1.45)$$

Results and discussion

The heat flow investigation of the mixtures CAC-10/0 and CAC-10/10 are shown in Figure 1a. The standard deviation for the heat of hydration after 22 h (H_{22h}) was determined from three independently measured sets of

data. In each case the plotted curves are the averaged curves. Both mixtures are characterised by an induction period between 0.5 and 1.5 h. The end of the induction period introduces the starting point of the main reaction. The maximum for both mixtures of 6 mW/g is very comparable. For the mixture without CA₂ (CAC-10/0), the heat flow after reaching the maximum, decreases down to the baseline. After 14 h the heat of hydration reaches a plateau at 67 J/g indicating the end of hydration. This compares with the mixture containing 10 wt.-% CA₂ which still releases a heat flow of 0.4 mW/g after 22 h. With 10 wt.-% CA₂ the heat of hydration is still increasing and has reached a value of 97 J/g after 22 h. As a consequence only through the addition of CA₂, a surplus of 30 J/g (45%) was achieved after a hydration time of 22 h.

The comparison of heat flow in CAC-10/10 and CAC-15/5 is shown in Figure 1b for a longer hydration time of 45 h. The mixture with 15 wt.-% CA and 5 wt.-% CA₂ (CAC-15/5) exhibits a much more pronounced main reaction than does the mixture with 10 wt.-% CA, with a significant maximum heat flow of 10.6 mW/g. After approximately 7 h the heat of hydration curve of CAC-15/5 exhibits a lower gradient than does the curve of CAC-10/10. After 33 h, however, the heat of hydration curves intersect one another. Finally CAC-10/10, the mix with lower CA content surprisingly releases more heat – 121 J/g after 45 h. Furthermore, the heat of hydration curves for both mixtures show that even after 45 h no plateau could be reached. This indicates that even after 45 h there is still some hydration reaction which is producing heat.

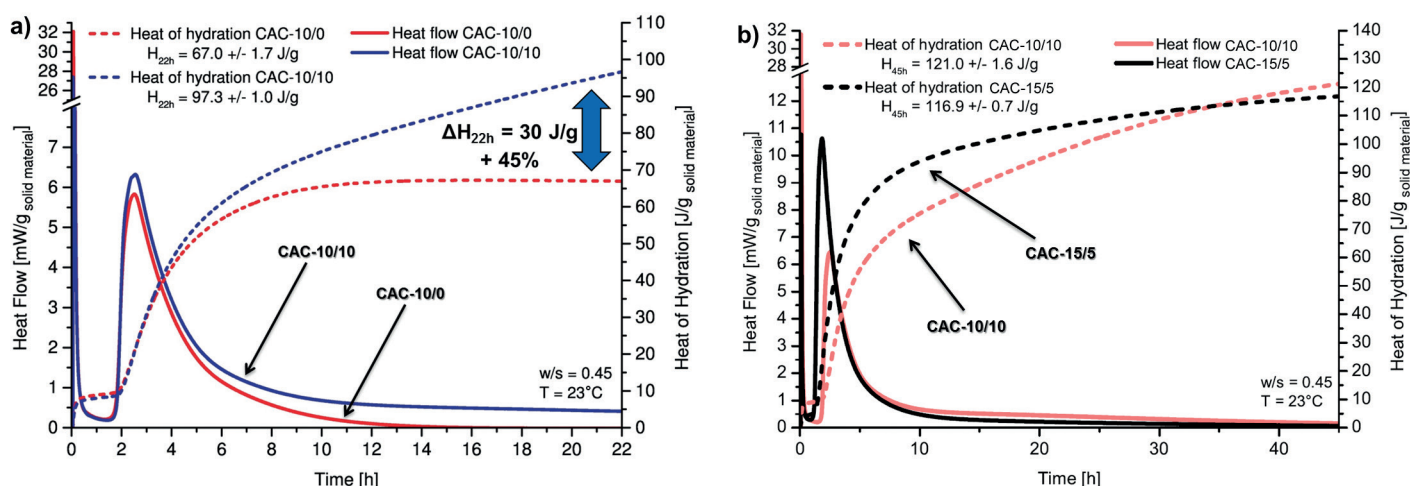


Figure 1: a) Heat flow (solid lines) and heat of hydration (dashed lines) for the mixtures CAC-10/0 (red) and CAC-10/10 (blue); b) Heat flow and heat of hydration for the mixtures CAC-10/10 (red) and CAC-15/5 (black); w/s = 0.45; T = 23°C

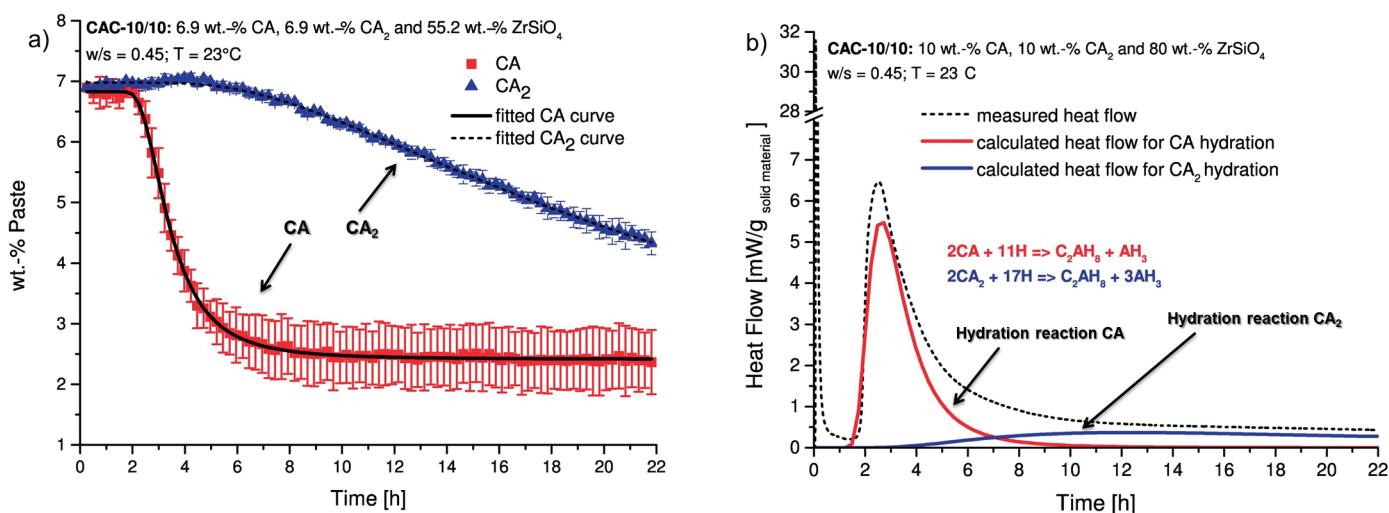


Figure 2: a) G-factor quantification of CA and CA₂ during hydration of the mixture CAC-10/10. b) Calculated heat flow for the hydration of CA and CA₂ in comparison with the measured heat flow; w/s = 0.45; T = 23°C

The G-factor quantification of CA and CA₂ during hydration of the mixture CAC-10/10 is shown in Figure 2a. After 1.75 h the main reaction starts with fast dissolution of CA. At the maximum of the main reaction, hydration of CA₂ is introduced after 4.5 h. The hydration rate of CA decreases after the main reaction and ceases after approximately 10 h. 2.5 wt.-% CA still remains after 22 h. In contrast, the dissolution of CA₂ proceeds continuously after the end of the measurement time.

Figure 2b shows the heat flow calculated from the QXRD data. The calculated heat flow for CA hydration according to reaction (1) starts after 1.75 h, at the same time as the measured heat flow. The maximum of the calculated heat flow of 5.5 mW/g is slightly lower than for the measured maximum. After the maximum, the calculated heat flow decreases and reaches the baseline after 10 h exhibiting no more heat for the rest of the measurement. The heat flow as calculated for hydration of CA₂ according to reaction (2) starts after the maximum of the CA hydration. As dissolution of CA₂ still occurs after 22 h, the heat flow is calculated to 0.3 mW/g at the end of the measurement.

Figure 3 shows the calculation of heat flow for the mixture with higher CA content. This is 15 wt.-% CA, 5 wt.-% CA₂ and 80 wt.-% ZrSiO₄ for a w/s of 0.45 at T = 23°C. The sum of the heat flow contributions based on the hydration reactions of CA and CA₂ is represented by the solid heat flow curve. The dashed line shows the heat flow as measured by the heat flow calorimetry.

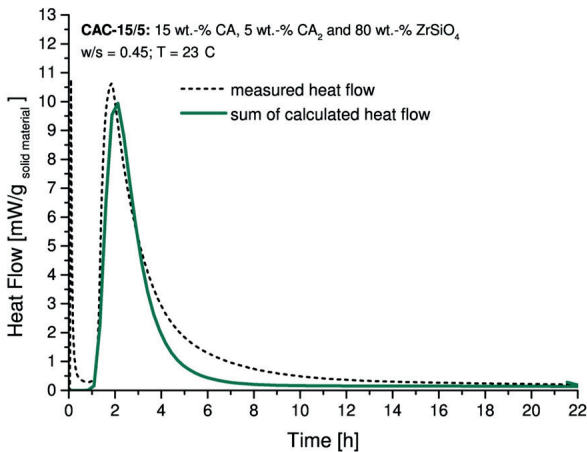


Figure 3: Calculation of heat flow for the mixture 15 wt.-% CA, 5 wt.-% CA₂ and 80 wt.-% ZrSiO₄ for a w/s of 0.45 at T = 23°C

Due to higher CA concentration the heat flow maximum after 2 h of 10.5 mW/g is more pronounced than for the mixture CAC-10/10 (compare Figure 2b). It then decreases slowly, finally reaching the baseline after approximately 16 h. Since the mixture CAC-15/5 contains only 5 wt.-% CA₂, the calculated heat flow based on the hydration reaction of CA₂ is quite low.

Figure 2 and Figure 3 underline the different behaviour in hydration kinetics of CA and CA₂. CA dissolves very rapidly once the main reaction has begun. The hydration of CA₂, on the other hand, is predominantly characterised by a very slow and lengthy reaction. Based on separate investigations it is known that CA₂ is completely dissolved after a few days.

The crystal structures of the hydrate phases C₂AH₈ and C₂AH_{7.5} are not yet sufficiently determined with regard to classical Rietveld refinement. For this reason hkl phases were used to fit the XRD pattern of C₂AH₈ and C₂AH_{7.5}. At 23°C aluminiumhydroxide is predominantly formed as AH_x-gel. For this reason AH₃ was not detectable with XRD.

The relative phase development of C₂AH₈ and C₂AH_{7.5} during the hydration of mixture CAC-10/10 is shown in Figure 4. The normalised scale factor

does not show any qualitative relationship but gives a hint on the phase kinetics. Precipitation of C₂AH₈ occurs as soon as the main reaction and CA dissolution has started. The amount of C₂AH₈ increases and reaches a maximum. After approximately 5 h of hydration the amount of C₂AH₈ decreases slowly. C₂AH_{7.5} is formed together with C₂AH₈ whereby the precipitation rate of C₂AH_{7.5} increases as soon as the amount of C₂AH₈ has reached its maximum. It is still in discussion whether C₂AH_{7.5} is formed through decomposition of C₂AH₈ or directly from solution. However, the formation of C₂AH_{7.5} can be supposed to contribute additional heat during CAC hydration reaction.

In Figure 2b and Figure 3 it can be noticed that the calculated heat flow is underdetermined during the deceleration period. As the formation of C₂AH_{7.5} was not taken into account during heat flow calculations, it can be assumed that the missing heat has its origin in C₂AH_{7.5} formation or conversion from C₂AH₈ to C₂AH_{7.5}.

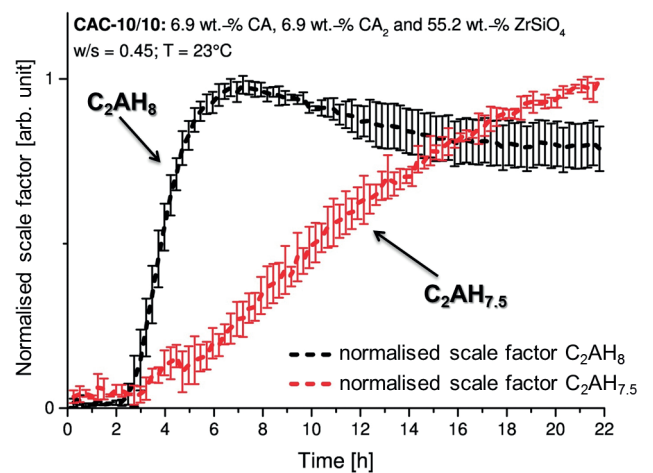


Figure 4: Phase development of the hydrate phases C₂AH₈ (black) and C₂AH_{7.5} (red) during hydration of the mixture CAC-10/10 for a w/s of 0.45 at T = 23°C

Practical relevance

In refractory applications, the assessment of strength development is often related to the main reaction (EXO max). However, the investigations show that considerable hydration takes place after the main reaction due to the CA₂ in CAC. Figure 5 shows the EXO curve and the strength development of a low cement tabular alumina vibration castable with dispersing alumina ADS/W after curing at 20°C for 5 h (EXO max), 24, 48, and 72 h. The cold crushing strength (CCS) increases from 26 MPa at 24 h to 35 MPa at 72 h (+ 35 %). This proves the significant contribution of CA₂ to the strength development if the curing time is long enough.

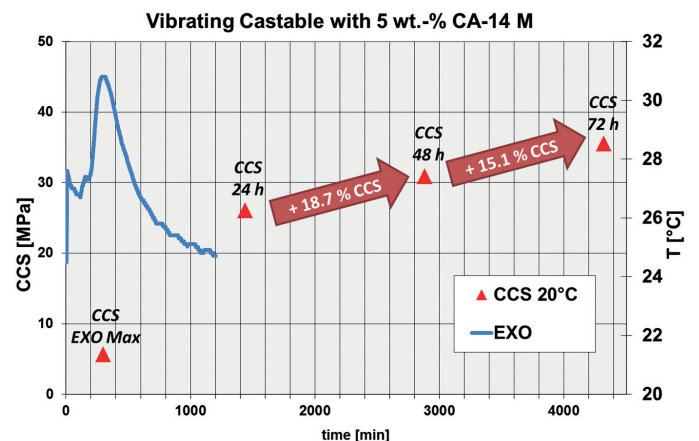


Figure 5: EXO measurement and curing strengths for a tabular alumina based vibrating castable with 5 wt.-% CA-14 M

Frequently performed on site installations may not permit such longer curing times. However for the production of large pre-cast shapes such as impact pads, steel ladle bottoms, or EAF delta sections a longer curing time would contribute to higher green strength. It would also reduce the risk of micro-cracking or more severe damage of the large pieces during de-moulding and handling.

Summary

A hydration model describing the different heat contributions is shown in Figure 6. It is very clear that once the hydration of CA has come to an end, remaining CA quantities in the paste do not contribute to further heat development. Additional heat is only developed through the ongoing hydration reaction of CA_2 and the phase conversion from C_2AH_8 to $C_2AH_{7.5}$.

It is shown by investigation of pure CA, and mixes of CA and CA_2 that the first reaction of CAC hydration is mainly influenced by the hydration of CA. The hydration of CA_2 begins as soon as the hydration of CA has reached its maximum rate. The dissolution of CA is accompanied by the precipitation of amorphous AH_x together with C_2AH_8 and $C_2AH_{7.5}$. The kinetics of CA_2 hydration is much slower than that for CA. The results very clearly show a pronounced influence of CA_2 on the hydration of CAC and its heat of hydration during the first 22 hours. After more than 10 h the CA_2 hydration gives the major heat contributions when compared to other reactions. It is obvious that the contribution of CA_2 to strength development cannot be neglected in refractory applications and that longer curing times would be beneficial especially for the production of large pre-cast shapes.

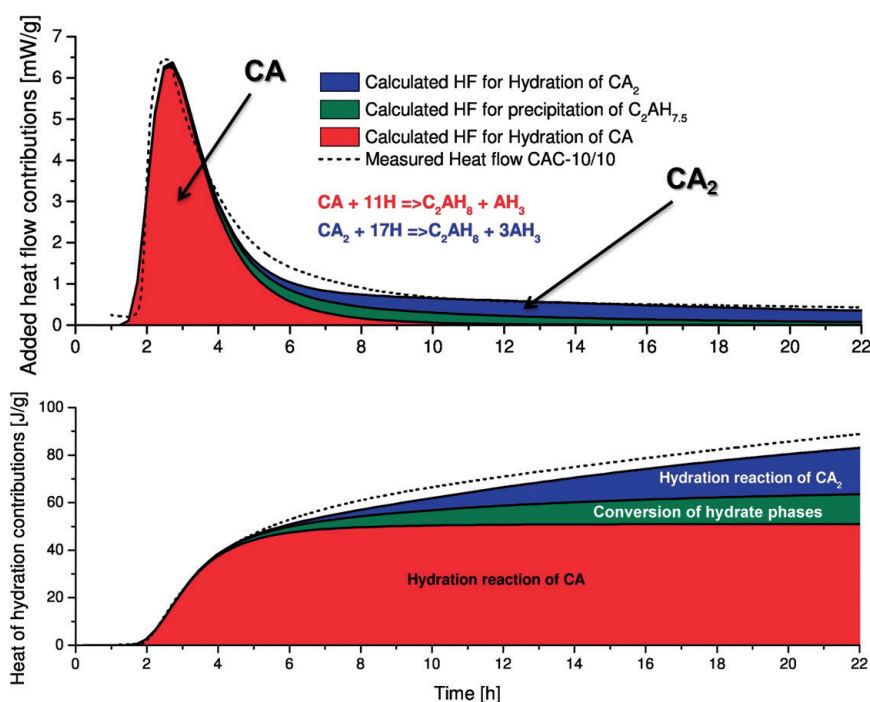


Figure 6: Hydration model describing the heat contributions during the hydration reaction of CAC based on the results of mixture CAC-10/10 at a w/s of 0.45 and a temperature of 23°C

Bibliography

- [1] S. Klaus, J. Neubauer and F. Goetz-Neunhoeffer, "How to increase the hydration degree of CA - The influence of CA particle fineness," *Cement and Concrete Research*, vol. 67, pp. 11-20, 2015.
- [2] D. Sorrentino, F. Sorrentino and M. George, "Mechanisms of hydration of calcium aluminate cements.," *Materials Science of Concrete*, vol. 4, pp. 41-90, 1995.
- [3] A. Buhr, D. Schmidtmeier, G. Wams, S. Kuiper and S. Klaus, "Testing of calcium aluminate cement bonded castables and influence of curing conditions on the strength development," in *Calcium Aluminates: Proceedings of the International Conference, Avignon, France*, 2014.
- [4] H. J. Kuzel, "An efficient conduction-type calorimeter.," *TIZ*, vol. 108, pp. 46-48, 50-51, 1984.
- [5] D. Jansen, C. Stabler, F. Goetz-Neunhoeffer, S. Dittrich and J. Neubauer, "Does Ordinary Portland Cement contain amorphous phase? A quantitative study using an external standard method.," *Powder Diffraction*, vol. 26, pp. 31-38, 2011.
- [6] S. Klaus, J. Neubauer and F. Goetz-Neunhoeffer, "Hydration kinetics of CA_2 and CA - Investigations performed on a synthetic calcium aluminate cement," *Cement and Concrete Research*, vol. 43, pp. 62-69, 2013.
- [7] H. M. Rietveld, "Profile refinement method for nuclear and magnetic structures.," *Journal of Applied Crystallography*, vol. 2, pp. 65-71, 1969.
- [8] S. T. Bergold, F. Goetz-Neunhoeffer and J. Neubauer, "Quantitative analysis of C-S-H in hydrating alite pastes by in-situ XRD.," *Cement and Concrete Research*, vol. 53, pp. 119-126, 2013.
- [9] B. H. O'Connor and M. D. Raven, "Application of the Rietveld refinement procedure in assaying powdered mixtures.," *Powder Diffraction*, vol. 3(1), pp. 2-6, 1988.
- [10] E. Prince, *International Tables for Crystallography, Volume C: Mathematical, Physical and Chemical Tables*, third edition ed., vol. C, Wiley, 2004, p. 1032.
- [11] M. Wojdyr, "Fityk: a general-purpose peak fitting program.," *Journal of Applied Crystallography*, vol. 43, pp. 1126-1128, 2010.
- [12] J. P. Coughlin, "Heats of formation of crystalline $CaO \cdot Al_2O_3$, $12CaO \cdot 7Al_2O_3$, and $3CaO \cdot Al_2O_3$.," *Journal of the American Chemical Society*, vol. 78, pp. 5479-82, 1956.
- [13] B. S. Hemingway, "Comment on "Thermodynamic properties of calcium aluminates",," *Journal of Physical Chemistry*, vol. 86, pp. 2802-3, 1982.
- [14] J. W. Johnson, E. H. Oelkers and H. C. Helgeson, "SUPCRT92: A software package for calculating the standard molal thermodynamic properties of minerals, gases, aqueous species, and reactions from 1 to 5000 bar and 0 to 1000°C.," *Computers & Geosciences*, vol. 18, pp. 899-947, 1992.
- [15] B. Lothenbach, T. Matschei, G. Moeschner and F. P. Glasser, "Thermodynamic modelling of the effect of temperature on the hydration and porosity of Portland cement.," *Cement and Concrete Research*, vol. 38, pp. 1-18, 2008.
- [16] T. Matschei, B. Lothenbach and F. P. Glasser, "Thermodynamic properties of Portland cement hydrates in the system $CaO-Al_2O_3-SiO_2-CaSO_4-CaCO_3-H_2O$.," *Cement and Concrete Research*, vol. 37, pp. 1379-1410, 2007.